Available online at www.sciencedirect.com
ScienceDirect
Catalysis Today 129 (2007) 200–206
CATALYSIS TODAY
www.elsevier.com/locate/cattod

Application of the Fenton process to the dissolution and mineralization of ion exchange resins

Monika Zahorodna [a], Romuald Bogoczek [a], Esther Oliveros [b,c,*], André M. Braun [b]

[a] *Katedra Technologii Chemicznej, Wydzial Inzynieryjno-Ekonomiczny, Akademia Ekonomiczna we Wroclawiu, 53345 Wroclaw, Poland*
[b] *Lehrstuhl für Umweltmesstechnik, Engler-Bunte Institut, Universität Karlsruhe, 76128 Karlsruhe, Germany*
[c] *Laboratoire des IMRCP, UMR CNRS 5623, Université Paul Sabatier, 31062 Toulouse Cédex 9, France*

Available online 17 September 2007

Abstract

Oxidative degradation of used ion exchange resins (IER) by the Fenton process is an attractive alternative to their deposition as hazardous waste. The process is leading to the dissolution of the polymer beads producing low molecular weight carboxylic acids and subsequently to their mineralization. Therefore, process development is focused for economic reasons at a fast dissolution of the polymer material, while keeping mineralization to a minimum. The optimal experimental design methodology (OED) was used to investigate the effects of primary reaction parameters (Fe(II)- and H_2O_2-concentrations and temperature) and to find the best parameter ranges for process optimization. The initial Fe(II)-concentration ($[Fe(II)]_0$) controlled the rate of dissolution, whereas H_2O_2-concentration and reaction temperature (40–60 °C) were found to be of minor impact. Spectrophotometric analysis demonstrated that an increase in $[Fe(II)]_0$ led to a fast decrease of the dissolution time (t_{dis}) as long as the concentration of Fe(II/III) was smaller than that needed for saturation of the IER. When the concentration of Fe(II/III) was higher than the capacity of the IER, efficient mineralization was found to take place. Oxidative degradation leading to the dissolution of the polymer beads is therefore most efficient as long as the catalyst is bound to the surface, whereas mineralization is most effective once the organic material is dissolved. This hypothesis is supported by REM images taken under different experimental conditions, as well as by the linear relation between the extent of mineralization and t_{dis}, in spite of the variation of the accessible surface of the polymer beads. An increase of the content of cross-linking agent affected adversely the oxidative degradation of the IER, mainly because it implies a diminution of the concentration of sulfonic acid groups and, hence, a decreased efficiency of iron complexation on the polymer beads.

Keywords: Ion exchange resins; Fenton reaction; Optimal experimental design

1. Introduction

Ion exchange resins (IER) based on copolymers of sulfonated styrene and divinylbenzene are widely used in the production of de-mineralized and de-ionized water, in the treatment of waste waters originating from, *e.g.* nuclear power stations or plating industries, for the recuperation of transition metal ions as well as for solid acid catalysts in epoxidation, esterification and inversion processes. However, IER are loosing progressively their original properties, and, as their chemical and physical deterioration progresses, they must be more or less frequently replaced. The principal cause of chemical deterioration is covalent bond breaking affecting primarily the functional groups, hence, leading to a diminution of their ion exchange capacity. In addition, covalent bond breaking may also imply the backbone of the copolymer diminishing the physical stability of the IER beads. Both processes might be due to degradation reactions induced by oxidizing agents present, *e.g.* in the aqueous medium to be treated, and are accelerated by elevated temperatures or the catalytic activity of metal ions [1]. Another kind of chemical deterioration might be due to additional cross-linking of the resin matrix that is initiated by sorbed species and results in a decrease of matrix flexibility and resin phase permeability, again affecting the physical stability of the resin beads [2]. Physical deterioration is mainly due to mechanical destruction of the resin beads during the great number of working cycles of IER under industrial conditions. All these processes are leading

* Corresponding author. Permanent address: Laboratoire des IMRCP, UMR CNRS 5623, Université Paul Sabatier, 31062 Toulouse Cédex 9, France.
E-mail addresses: Monika.Zahorodna@ae.wroc.pl (M. Zahorodna), Esther.Oliveros@ciw.uni-karlsruhe.de, oliveros@chimie.ups-tlse.fr (E. Oliveros).

0920-5861/$ – see front matter © 2007 Elsevier B.V. All rights reserved.
doi:10.1016/j.cattod.2007.08.014

to decreased selectivity and capacity as well as to increased difficulties in the technical handling of IER. At present, used IER are considered to be useless waste material, and spent IER are mostly deposited in landfill sites.

Different processes were proposed and investigated for disposing of IER, *e.g.* incineration [3], thermal decomposition [4–6], acid ''digestion'' [7], as well as wet oxidation [8].

Only a few results are known concerning a controlled (partial) oxidation of polystyrene based IER by hydrogen peroxide (H_2O_2) and catalyzed by transition metal ions (Fenton or Fenton-like processes, [9]). In most cases, authors analyzed the progressively reduced capacities of the oxidized IER [10,11], but in more recent publications, rates of carbon dioxide (CO_2) [12,13] and sulfate (SO_4^{2-}) evolution [14] were investigated. According to these authors, Fenton-type oxidation processes lead to the destruction of the cross-linked structure of the IER and to partially desulfonated products of lower molecular weight. However, such oxidative degradation might not only be used to solve an environmental problem, a controlled oxidation process might also be focused on introducing polar functions (alcohol, carbonyl and carboxylic acid) to partially degraded or desulfonated polymers, hence producing new soluble products of potential use, *e.g.* as polyelectrolytes.

Oxidative degradation of polymer surfaces is best initiated by hydroxyl radicals ($HO^{\bullet}$), as generated in most advanced oxidation processes (AOP). Given the metal ion coordinating properties of the IER, Fenton or Fenton-type processes [9] might not only be best suited for that purpose, their investigation might also provide important mechanistic information. As far as a technical development is concerned, the use of the Fenton reagent ($Fe(II)/H_2O_2$, Eq. (1)) as an oxidant is attractive, since iron is inexpensive and non-toxic, and aqueous solutions of hydrogen peroxide are of no environmental concern.

$$Fe(II) + H_2O_2 \rightarrow Fe(III) + HO^- + HO^{\bullet} \quad (1)$$

In the present work, dissolution and mineralization of IER using the Fenton process were investigated, and, aiming at a most economic procedure, process conditions were optimized for short reaction times for complete dissolution of the IER particles, while keeping the rate of mineralization at a minimum. The experimental design methodology was used for planning the series of experiments under normalized conditions and for simulating and predicting IER dissolution times and rates of mineralization as a function of the three main factors: Fe(II) and H_2O_2 concentrations and temperature.

2. Materials and methods

2.1. Reagents

All reagents and solvents used were of the highest purity available. The ion exchange resin Amberjet 10.5 1500 H (Rohm & Hass) in its protonated form was purified by washing twice with 1 M HCl and four times with water and subsequent drying in air for 2 weeks. This resin consists of fully protonated sulfonated polystyrene cross-linked with divinylbenzene (elemental analysis: 38.94% C, 5.90% H, 11.98% S; capacity indicated by provider: 4.2 mval/g). The IER used in this work contained 26.83% of H_2O in weight.

$Fe(SO_4)\cdot 7H_2O$ (98%, Aldrich), H_2O_2 (30%, w/w H_2O_2 in water, Roth), conc. HCl and conc. H_2SO_4 (Merck) were used as purchased. H_2O_2 was analyzed by $KMnO_4$ titration. Reagents and solvents used for UV/vis spectroscopy, HPLC and IC (Section 2.3) were also purchased from Merck and used as supplied. H_2O was of tri-distilled quality (UHQ-II).

2.2. Experimental procedure

The experiments were conducted in the dark in an airtight glass vessel of 1L capacity. An aqueous solution (100 mL) of catalyst ($Fe(SO_4)\cdot 7H_2O$), in the range from 2.0 to 20.0 mM, was introduced into the reactor and thermoregulated at the desired temperature. The initial pH value of the solution was adjusted to 3 using H_2SO_4. In a first series of experiments, the ion exchange resin (1 g) was added just before starting addition of H_2O_2, whereas in a second series of experiments, the reaction mixture was stirred for 15 min before starting addition of H_2O_2. An aqueous solution of H_2O_2 at constant concentration (15%) was added continuously at a flow rate varying between 0.5 and 2.5 mL min^{-1} until all IER particles were dissolved (t_{dis}). During the reaction, the mixture was stirred and constantly saturated with synthetic air (45 mL min^{-1}).

2.3. Analytical techniques

The extent of mineralization of the IER was determined as the weight of $CaCO_3$ (W [mg]) produced by trapping CO_2 emerging from the acid reaction medium in a saturated $Ca(OH)_2$ solution. $CaCO_3$ was filtered and dried at 70 °C during 12 h.

The quantitative analysis of SO_4^{2-} (formed as a result of the degradation of sulfonated polystyrene) was carried out by ion chromatography (IC, Dionex-DX 500, column: Ion Pac AS-14, 250 mm, eluent: 3.5 mM Na_2CO_3 and 1.0 mM $NaHCO_3$ in tri-distilled water, isocratic, flow rate: 1.2 mL min^{-1}, detection: 285 nm). Samples were periodically taken from the reactor and filtered through a nylon filter of 0.2 μm (Roth) before injection.

Analysis of the main intermediates resulting from the degradation of the IER was carried out by liquid chromatography (HPLC or IC) in an isocratic mode. The system was equipped with a L-7455 Merck UV/vis detector. Different columns and eluents were used for separation and identification of the compounds.

For sulfonic intermediates (acids): column: Knauer C18 (250 mm), eluent: 70/30 (v/v) water/methanol with 5 mM of tetrabutylammonium hydrogensulfate, flow rate 1 mL min^{-1}, detection: 254 nm. For phthalic and benzoic acids: Knauer C18 (250 mm), eluent: methanol/20 mM phosphoric acid (40/60, v/v), flow rate: 1 mL min^{-1}, detection: 210 nm. For oxalic and maleic acids: column: Knauer C8 (250 mm), eluent: 0.1 M KH_2PO_4/acetonitrile (90/10, v/v), flow rate: 2 mL min^{-1}, detection: 210 nm) and for formic and acetic and succinic

acids: column: Hamilton PRP X-300 (150 mm), eluent: 1 mN H_2SO_4, flow rate: 2 mL min^{-1}, detection: 210 nm.

Adsorption (complexation) of Fe(II) and Fe(III) onto the IER was determined by spectrophotometric analysis (Varian, Cary 500). An aqueous solution (100 mL) of catalyst ($Fe(SO_4)\cdot 7H_2O$), in the range from 2.0 to 20.0 mM, was introduced into the reactor and thermoregulated at the desired temperature. The initial pH value of the solution was adjusted to 3 using H_2SO_4. After the IER (1 g) was added, samples (2.0 mL) were taken periodically and filtered through 0.2 μm nylon filters (Roth). 1.5 mL of a reagent solution consisting of 0.10 M of 1,10-phenanthroline in 0.10 M of an acetic acid/acetate buffer were added to the filtered sample to obtain $[Fe(phen)_3]^{2+}$ which was analyzed by its absorption at $\lambda_{max} = 510$ nm ($\varepsilon = 11{,}100\ M^{-1}\ cm^{-1}$). For the analysis of Fe(III), 1.5 mL of a solution of 0.10 M of aqueous NH_4SCN was added to the sample to obtain $[Fe(SCN)_2(H_2O)]^+$ which was analyzed by its absorption at $\lambda_{max} = 473$ nm ($\varepsilon = 8800\ M^{-1}\ cm^{-1}$). All analyses were made using tri-distilled H_2O as a reference, and in both cases, linear calibration curves were obtained.

2.4. Optimal experimental design

The experimental design methodology (OED) was used for planning the experimentation and for analyzing the experimental results [15–18]. This methodology is based on multivariate methods where the levels (settings or values) of the independent variables (*e.g.* processing conditions) are simultaneously modified from one experiment to another. It provides the means of building a statistically significant model of a phenomenon by performing a minimum set of experiments adequately distributed in the experimental region (experimental matrix). A large number of experimental designs adapted to various types of problems are available, such as factorial designs, centroid composite matrices, Doehlert arrays [15,19]. In these designs, each independent variable U_i is associated with a normalized variable, usually a reduced and centered variable X_i (Eq. (2)).

$$X_i = \frac{U_i - U_{i,0}}{\Delta U_i} \tag{2}$$

where $U_{i,0}$ ($=(U_{i,max} + U_{i,min})/2$) is the value of U_i at the centre of the experimental region, ΔU_i ($=(U_{i,max} - U_{i,min})/2$) is the step with $U_{i,max}$ and $U_{i,min}$ maximum and minimum values of the effective variable U_i, respectively.

For this work, Doehlert uniform arrays [16,20,21] were chosen as experimental matrices. The experimental responses of interest (dependent variables $Y = f(X_i)$) associated to such type of matrices are represented by quadratic polynomial models (Eq. (3) for 2 variables).

$$Y = b_0 + b_{i1}X_1 + b_2X_2 + b_{11}X_1^2 + b_{22}X_2^2 + b_{12}X_1X_2 \tag{3}$$

The least-square estimates of the coefficients of the model (b_i) were calculated from the values of the response Y for each experiment in the chosen experimental matrix. The resulting model allows the drawing of contour plots (lines or curves of constant response value, *e.g.* Fig. 2) and of three-dimensional representations of the response (not shown in this publication). The experiment at the centre of the Doehlert array is usually run in triplicate in order to check the reproducibility and to obtain an estimate of the standard deviation of the experimental response Y. The validity of the model was checked in performing control experiments inside the experimental region.

In a first step, a Doehlert matrix for 2 variables was used for investigating the effects of the initial Fe(II) concentration ($[Fe(II)]_0$) and of the rate of addition of the H_2O_2 solution ($[H_2O_2]$) on the two responses of interest, the dissolution time (t_{dis}) and the extent of mineralization ($W(CaCO_3)$). This matrix contains 7 uniformly distributed experiments that may be represented by the apexes and centre of a hexagon (Table 1, experiments 1–6 and 13). In a second step, a third variable (temperature) was introduced by adding 6 experiments (Table 1, experiments 7–12), resulting in a matrix containing 13 experiments that may be represented by the apexes and centre of a cube octahedron [22]. The experimental responses of interest Y are represented by Eq. (4).

$$Y = b_0 + b_1X_1 + b_2X_2 + b_3X_3 + b_{11}X_1^2 + b_{22}X_2^2 + b_{33}X_3^2 + b_{12}X_1X_2 + b_{13}X_1X_3 + b_{23}X_2X_3 \tag{4}$$

The NEMROD software [23] was employed for calculating the coefficients of the polynomial models representing the variations of the responses (Eqs. (3) and (4)), as well as for drawing the corresponding contour plots (Fig. 1).

3. Results and discussion

3.1. Process modeling using optimal experimental design

As already noted in previous investigations [9,24], Fe(II/III) and H_2O_2 concentrations are the primary parameters affecting the rate of oxidation of organic substrates in Fenton processes. The variation of the H_2O_2 concentration was achieved by controlling the rate of addition of a 15% H_2O_2 solution to a suspension of IER (Amberjet 10.5 1500 H) in a Fe(II) solution of defined initial concentration and pH-value. The ranges of variation of the variables, as well as the amount of IER to be oxidized, were chosen from exploratory studies. The experimentation was planned according to the experimental design methodology and was based on Doehlert matrices (Section 2.4). The corresponding set of experiments and the values of the experimental responses (dissolution time (t_{dis}) and extent of mineralization (represented by the amount of $CaCO_3$ formed until t_{dis} ($W(CaCO_3)$, s. §2.3) are listed in Table 1. The extent of mineralization was also calculated as % of the initial TOC value. During the experiments, the pH-value of the reaction system decreased by 1 to 1.5 units. Equilibration of the suspended IER with the Fe(II) solution (15 min of stirring) before adding H_2O_2 yielded within limits of error the same results as the experiments, without previous equilibration (§ 2.2).

Table 1
Values of effective (U_i) and normalized (X_i) variables and corresponding experimental responses, t_{dis}, $W(CaCO_3)$ and % of initial TOC mineralized until t_{dis}, for the experiments contained in the Doehlert uniform array used in this work

Exp. no.	U_1 [H_2O_2] (mL min^{-1})	U_1 H_2O_2 (mol min^{-1})	U_2 [Fe(II)] (mM)	U_3 T (°C)	X_1	X_2	X_3	t_{diss} (min)	$W(CaCO_3)$ (mg)	Initial TOC[a] mineralized%
1	2.5	12.125×10^{-3}	11.0	50	1	0	0	25	204	8.6
2	0.5	2.425×10^{-3}	11.0	50	−1	0	0	77	322	13.5
3	2.0	9.7×10^{-3}	20.0	50	0.5	0.866	0	26	424	17.8
4	1.0	4.85×10^{-3}	2.0	50	−0.5	−0.866	0	166	100	4.2
5	2.0	9.7×10^{-3}	2.0	50	0.5	−0.866	0	161	53	2.2
6	1.0	4.85×10^{-3}	20.0	50	−0.5	0.866	0	45	429	18.0
7	2.0	9.7×10^{-3}	14.0	60	0.5	0.288	0.816	24	211	8.9
8	1.0	4.85×10^{-3}	8.0	40	−0.5	−0.288	−0.816	77	110	4.6
9	2.0	9.7×10^{-3}	8.0	40	0.5	−0.288	−0.816	58	65	2.7
10	1.5	7.275×10^{-3}	17.0	40	0	0.577	−0.816	31	177	7.4
11	1.0	4.85×10^{-3}	14.0	60	−0.5	0.288	0.816	36	263	11.1
12	1.5	7.275×10^{-3}	5.0	60	0	−0.577	0.816	33	103	4.3
13[b]	1.5	7.275×10^{-3}	11.0	50	0	0	0	32[c]	179[c]	7.5
14[d]	2.0	9.7×10^{-3}	16.2	50	0.5	0.5	0	24 (18)	264 (285)	11.1(12.0)
15[d]	2.0	9.7×10^{-3}	6.5	50	0.5	−0.5	0	48 (57)	101 (90)	4.2 (3.8)

[a] Average intial TOC value: 0.289 g C g^{-1} IER (100%).
[b] Experiment at the centre of the experimental region (average of three repetitions), denoted as 0 in Fig. 1.
[c] Standard deviation: 3 min for t_{dis} and 12 mg for $W(CaCO_3)$.
[d] Control experiments (values predicted by the model are given in parentheses).

Under the experimental conditions chosen, the minimum value of t_{dis} was found in the upper right quadrangle of the contour plot (Fig. 1a), at a relatively high rate of H_2O_2 addition and a $[Fe(II)]_0$ between 11 and 21.4 mM. The contour plot shows that the rate of H_2O_2 addition was of practically no effect at $[Fe(II)]_0 < 11$ mM. In contrast, t_{dis} decreased very rapidly with increasing $[Fe(II)]_0$ until a value of approx.11 mM was reached, and a rather flat response was observed for $[Fe(II)]_0 > 11$ mM.

These observations might be interpreted by taking into account the capacity of the IER used in this work (3.07 mval/g (corrected for water content, § 2.1), meaning that 1 g of IER would be saturated by 100 mL of an aqueous solution of 15 mM of Fe(II)). Spectrophotometric analysis of the complexation of iron ions by the IER (§ 2.3) showed that, as long as the concentration of Fe(II) was smaller than that needed for saturation, Fe(II) was practically quantitatively bound to the IER (≥99% determined for 14 mM of Fe(II) after 7, 11 and 30 min, Fig. 2). In fact, values of absorbance did not vary for more than 0.01 units after 7 min. Under these conditions, the Fenton reaction should take place almost exclusively at the IER surface and an increase in $[Fe(II)]_0$ from its minimum value to IER saturation should lead to a decrease of t_{dis}. In fact, t_{dis} was observed to decrease very fast (from approx. 160 to 24 min) when $[Fe(II)]_0$ was increased from 2 up to 14 mM, showing that the IER-bound catalyst was most effective for the oxidative degradation and dissolution of the polymer beads.

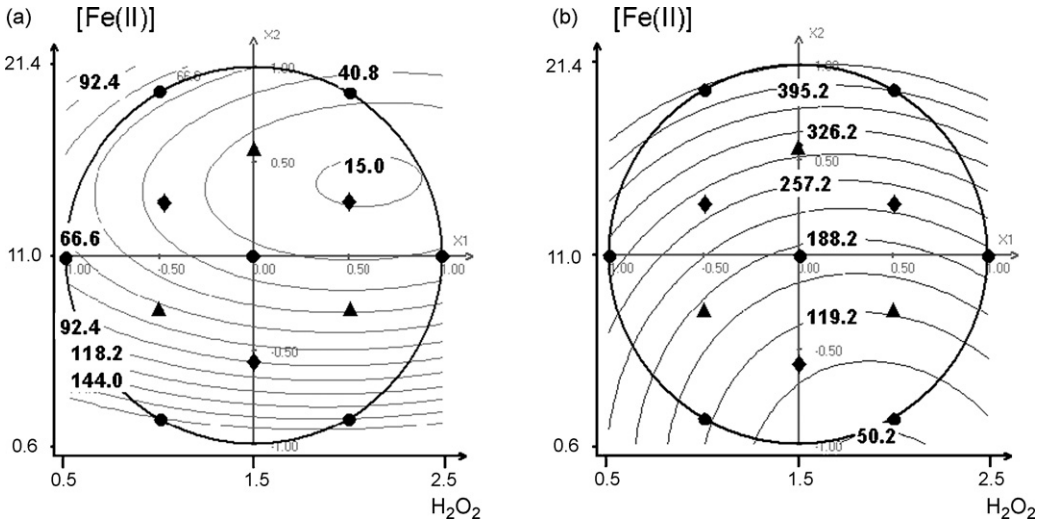

Fig. 1. Contour plots representing the effects of the initial concentration of Fe(II) (mM) and of the rate of H_2O_2 addition (mL min^{-1}) on (a) the IER dissolution time (t_{dis} (min), bold numbers), and (b) mineralization ($W(CaCO_3)$ (mg), bold numbers) at 50 °C. The different symbols represent experiments at 40 °C (▲), 50 °C (●) and 60 °C (◆). Grey numbers represent the values of the normalized variables X_1 and X_2.

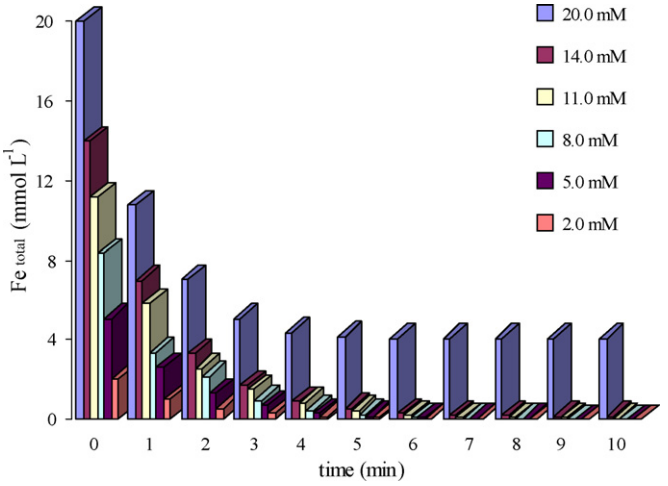

Fig. 2. Evolution of the concentration of Fe(II) in an aqueous solution (100 mL) upon suspending 1 g of IER (Amberjet 10.5 1500 H); [Fe(II)] = 2–20 mM, 50 °C.

When the $[Fe(II)]_0$ was increased above the IER capacity (14–21.4 mM), the concentration of Fe(II) ions in solution increased, however, t_{dis} was not so much affected (Fig. 1a). This means that an increased hydroxyl radical ($HO^\bullet$) generation in the bulk aqueous phase (Eq. (1) did not contribute significantly to the IER dissolution. This result suggests that the diffusion to and reaction of $HO^\bullet$ with the polymer surface is slower than the lifetime of the radical. The increase of t_{dis} at $[Fe(II)]_0 > 16$ mM might even indicate that known competing reactions, such as (5) and (6) are gaining in importance.

$$Fe(II) + HO^\bullet \rightarrow Fe(III) + HO^- \quad (5)$$

$$HO^\bullet + H_2O_2 \rightarrow H_2O + HO_2^\bullet \quad (6)$$

Focusing on either minimum costs or on the use of the Fenton process for the production of material of potential use, *e.g.* as polyelectrolytes, mineralization should be kept at a minimum. The contour plot for the extent of mineralization ($W(CaCO_3)$) until t_{dis} (Fig. 1b) shows that the minimum region is located in the lower right quadrangle with a minimum value at the limit of the experimental region, *i.e.* at $[Fe(II)]_0 \leq 0.8$ mM. As in the case of t_{dis}, mineralization is primarily controlled by the initial amount of Fe(II) ions, but, in contrast to t_{dis}, a smooth increase is observed as $[Fe(II)]_0$ increases, without any particular behavior related to the IER capacity ($[Fe(II)]_0 \geq 14$ mM). This result may be an indication that mineralization is taking place mainly in solution. However, as this response is integrating CO_2 production during the whole dissolution process, several effects have to be taken into account: (1) oxidation of the IER surface, (2) dissolution of the polar polymer fragments produced and their subsequent further oxidation and mineralization in solution, (3) decomplexation and desorption of Fe(II/III) as IER degradation progresses and 4) complexation of Fe(III) (Eq. (1)) in solution by carboxylic acids (§ 2.3), *e.g.* oxalic acid.

As expected, for both, the dissolution and the mineralization processes, the effect of the reaction temperature was rather limited in the range investigated (40–60 °C). In the case of t_{dis}, a shift of the minimum toward the centre of the experimental region could be observed with increasing temperature (results not shown).

As the minima of t_{dis} and of ($W(CaCO_3)$ are not at the same location in the experimental region, a compromise has to be sought. For example, if a $[Fe(II)]_0$ of approx. 11 mM and a rate of H_2O_2 addition of approx. 2.0 mL min^{-1} are employed at a reaction temperature of 60 °C, a t_{dis} of 15 min and a ($W(CaCO_3)$) of approx. 6% of the TOC suspended are predicted by the model. Test experiments 14 and 15 (see Table 1) show that predicted values of t_{dis} and ($W(CaCO_3)$) are met experimentally within a limit of error of less than 15%.

3.2. Effect of cross-linking and particle size

Experiments discussed above were made with a sulfonated polystyrene copolymerized with 10.5% of divinylbenzene (DVB). Following the hypothesis that the oxidative degradation of the IER beads is most effectively initiated by the Fenton reaction of surface bound Fe(II) ions, a variation of the contents of cross-linking agent should also effect the oxidative degradation of the organic substrate, because the IER would change their chemical (accessible surface concentration of sulfonic acid groups) as well as their physical (porosity, swelling, etc.) characteristics. An increase of the content of cross-linking agent would also lead to the diminution of sulfonate functionalization and, hence, to a decreased efficiency of iron complexation. Consequently, a higher content of cross-linking agent should effect adversely the oxidative degradation of the IER, and indeed t_{dis} was found to increase, when the amount of DVB in the IER increased (Fig. 3). With $[Fe(II)]_0 = 16.2$ mM, saturation of the IER was ensured for all copolymers investigated, and the effect can only be explained by the accessible concentration of Fe(II) complexing sites.

The reported dependence of mineralization on the amount of cross-linking agent (Fig. 3) is most probably due to the time of reaction (t_{dis}) increasing with the amount of cross-linking agent, since this response was always determined at t_{dis}.

The dissolution time (t_{dis}) was observed to increase with increasing bead diameter, under otherwise identical conditions ($[Fe(II)]_0 = 16.2$ mM, 2 mL min^{-1} H_2O_2, 50 °C, 1 g of IER)

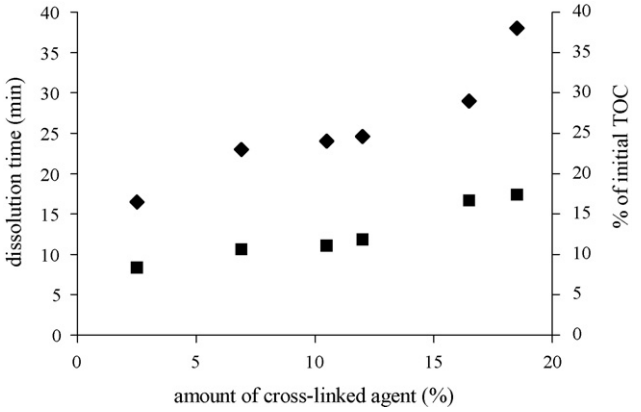

Fig. 3. Dissolution time (t_{dis}) (◆) and extent of mineralization until t_{dis} (■) determined for sulfonated polystyrenes copolymerized with different amounts of divinylbenzene. $[Fe(II)]_0 = 16.2$ mM, 2 mL min^{-1} H_2O_2 (15%), 50 °C.

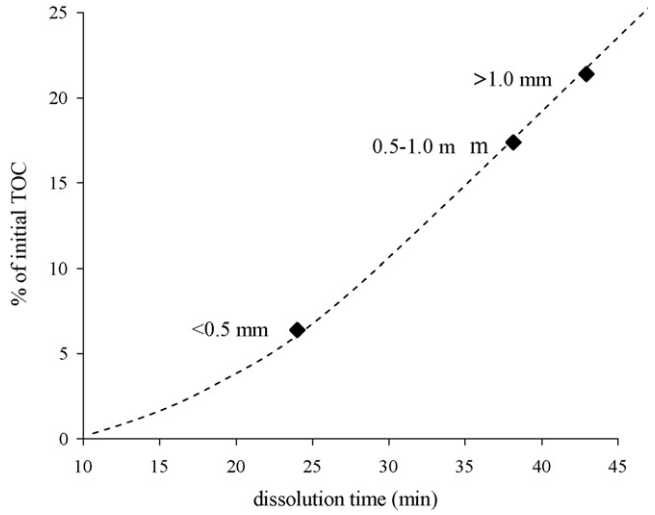

Fig. 4. Extent of mineralization vs. dissolution time (t_{dis}) for IER beads of different diameter; $[Fe(II)]_0$ = 16.2 mM, 2 mL min^{-1} H_2O_2, 50 °C.

(Fig. 4). If it is assumed that the IER dissolution is due primarily to the Fenton reaction taking place at the interface between the bulk solution and the polymer beads (*i.e.* between H_2O_2 and surface bound Fe(II)), the rate of dissolution (r_{dis}) should be proportional to the total surface area of suspended IER particles. The latter being dependent on the inverse of the particle radius for a given total weight of suspended material, r_{dis} should decrease when the particle diameter decreases, and therefore, t_{dis} should increase with particle diameter (as observed, Fig. 4).

The extent of mineralization also increased with particle size (Fig. 4) and therefore with reaction time (=t_{dis}). Interestingly, a linear relation was observed between the extent of mineralization and t_{dis}, which might be interpreted as an indication of the dominant mineralization of dissolved organic fragments. In fact, larger beads need more time to be degraded to dissolution (t_{dis}), and since the reaction time for the mineralization process increases with t_{dis}, higher values of $W(CaCO_3)$ are reached.

The degradation of the IER beads by the Fenton process may be visualized by REM images. For conditions where $[Fe(II)]_0$ = 2 mM and, hence, far below IER saturation, constant bead size was still observed after 100 min of reaction time (t_{dis} = 160 min), but polymer degradation is clearly visible, as the surface is locally swollen and disintegrating (Fig. 5a). Moreover, apparently solidified outflows of partially degraded (and not yet soluble) material can be observed (Fig. 5b). Under conditions of $[Fe(II)]_0$ = 20 mM, *i.e.* beyond IER saturation, the absence of these outflows might be due to rapid oxidation and dissolution of such partially degraded material (Fig. 5c). Moreover, a modification of the surface might have led to the clearly visible adhesion between individual beads. In addition, the bead size was found to decrease and vary considerably after 15 min of reaction time (t_{dis} = 24 min; the untreated beads are

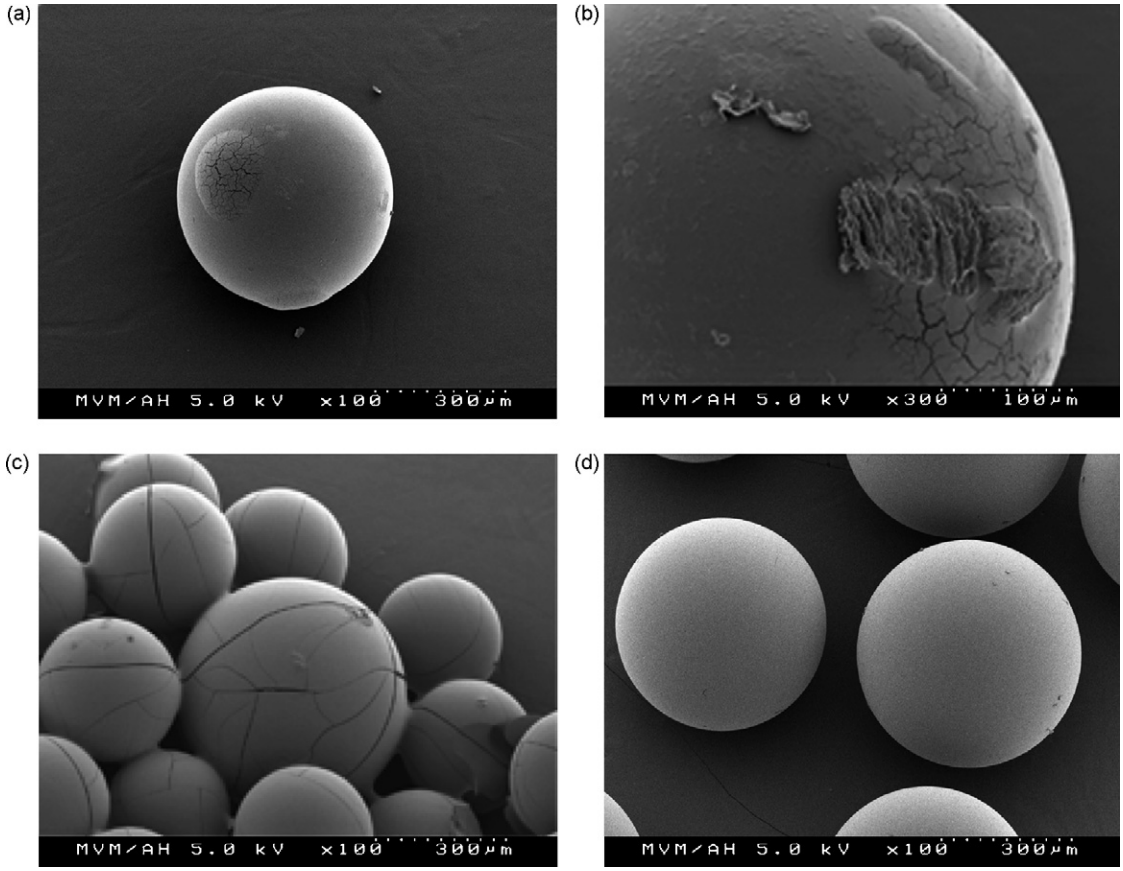

Fig. 5. REM-images of partially oxidized IER beads (Amberjet 10.5 1500 H); (a, b) $[Fe(II)]_0$ = 2 mM, 2 mL min^{-1} H_2O_2, 50 °C, reaction time: 100 min; (c) $[Fe(II)]_0$ = 20 mM, 2 mL min^{-1} H_2O_2, 50 °C, reaction time: 15 min, (d) unused IER beads.

shown for comparison (Fig. 5d)). It should be noted that particles remained spherical during the dissolution process, confirming the importance of surface reactions.

As expected, the Fenton process did not lead to the complete mineralization of the IER. It is known that, Fe(III) formed in the Fenton reaction (Eq. (1)) is complexed by the carboxylic acids resulting from the oxidation process [9,24], preventing reduction of Fe(III) by H_2O_2 (Eq. (7)) and thus recycling of Fe(II).

$$\mathrm{Fe(III)} + \mathrm{H_2O_2} \rightarrow \mathrm{Fe(II)} + \mathrm{H^+} + \mathrm{HO_2^\bullet} \quad (7)$$

In the case of the IER, even for $[Fe(II)]_0$ far below exchange capacity, complete dissolution of the beads is achieved, indicating that Fe(III) bound to the IER surface may be reduced to Fe(II) (Eq. (7)). This indicates that oxidation of IER beads up to the carboxylic acid stage is not occurring on the particles, because if this would be the case, Fe(III) would be irreversibly complexed and not available for recycling; consequently, complete dissolution could not be reached.

As shown for a number of organic compounds [9], the extent of mineralization of the IER can be increased under irradiation, due to the reduction of Fe(III) to Fe(II) by photolysis of the Fe(III)-complexes with low molecular weight carboxylic acids. The presence of such Fe(III)-complexes was confirmed spectrophotometrically, and the photochemically enhanced Fenton process led to a sharp increase of the mass of CO_2 due to mineralization of the IER (results to be published).

Acknowledgments

M.Z. is grateful to the Deutscher Akademischer Austauschdienst (DAAD) and to the Auslandsamt of the University of Karlsruhe for personal grants enabling her to realize this part of her PhD thesis at the University of Karlsruhe.

References

[1] L.F. Wirth, C.A. Feldt, K. Odland, Ind. Eng. Chem. 53 (1961) 638.
[2] A.A. Zagorodni, D. Kotova, V.F. Selemenev, React. Funct. Polym. 53 (2002) 157.
[3] K. Kinoshita, M. Hirata, T. Yahata, J. Nucl. Sci. Technol. 28 (1991) 228.
[4] M.A. Dubois, J.F. Dozol, C. Nicotra, J. Serose, C. Massiani, J. Anal. Appl. Pyrol. 31 (1995) 129.
[5] U.K. Chun, K. Choi, K.H. Yang, J.K. Park, M.J. Song, Waste Manag. 18 (1998) 183.
[6] R.S. Juang, T.S. Lee, J. Hazard. Mater. B92 (2002) 301.
[7] Y. Kabayashi, H. Matsuzuru, J. Akatsu, N. Moriyama, J. Nucl. Sci. Technol. 17 (1980) 865.
[8] M.A. Dubois, J.F. Dozol, C. Massiani, M. Ambrosio, Ind. Eng. Chem. Res. 35 (1996) 2743.
[9] J.J. Pignatello, E. Oliveros, A. MacKay, Crit. Rev. Environ. Sci. Technol. 36 (2005) 1.
[10] W. Wood, J. Phys. Chem. 61 (1957) 832.
[11] L.S. Goldring, International Conference on the Theory and Practice of Ion Exchange, Churchill College, University of Cambrige, 1976, paper 7.1.
[12] X. Jian, T. Wu, G. Yun, Nucl. Safety 37 (1996) 149.
[13] P.A. Taylor, ORNL/TM-2002/197, Oak Ridge National Laboratory, Oak Ridge, 2002, p. 1.
[14] M. Kubota, J. Radioanal. Chem. 78 (1983) 295.
[15] A.I. Khuri, J.A. Cornell, Response Surfaces, Designs and Analyses, Marcel Dekker, New York, 1987.
[16] E. Oliveros, O. Legrini, M. Hohl, T. Mueller, A.M. Braun, Chem. Eng. Process. 36 (1997) 397.
[17] D. Rasch, L.R. Verdooren, J.I. Gowers, Fundamentals in the Design and Analysis of Experiments and Surveys, in: Grundlagen der Planung und Auswertung von Versuchen und Erhebungen, Oldenbourg Wissenschaftsverlag, München, 1999.
[18] S. Göb, E. Oliveros, S.H. Bossmann, A.M. Braun, Water Sci. Technol. 44 (2001) 339.
[19] A.C. Atkinson, Optimum Experimental Design, Clarendon, Oxford, 1992.
[20] G. Dumenil, G. Mattei, M. Sergent, J.C. Bertrand, M. Laget, R. Phan Tan Luu, Appl. Microbiol. Biotechnol. 27 (1988) 405.
[21] F. Benoit-Marquié, E. Costes-Puech, A.M. Braun, E. Oliveros, M.T. Maurette, J. Photochem. Photobiol. A: Chem. 108 (1997) 65.
[22] E. Oliveros, S. Göb, S.H. Bossmann, A.M. Braun, C.A.O. Nascimento, R. Guardani, Sustainable Energy and Environmental Technology, in: X. Hu, P.L. Yue (Eds.), Proceedings of the Third Asia Pacific Conference, World Scientific, Singapore, (2000), p. 577.
[23] NEMROD version 2002, LPRAI, B.P. no 7, Marseille, Le Merlan, 13311 Marseille Cédex 14, France.
[24] S.H. Bossmann, E. Oliveros, S. Göb, S. Siegwart, E.P. Dahlen, L. Payawan Jr., M. Straub, M. Wörner, A.M. Braun, J. Phys. Chem. A 102 (1998) 5542.